

Automated Preliminary Thermal and Stress Analyses Applied to a Turbine Housing Assembly

M. Moret¹, H. Moustapha¹, Patricia Phutthavong², F. Garnier^{1,*}

¹Ecole de Technologie Supérieure, Montreal, Quebec, Canada

²Pratt & Whitney Canada, Montreal, Quebec, Canada

Abstract The use of Multidisciplinary Design Optimization (MDO) techniques at the preliminary design phase (PMDO) of a gas turbine engine allows investing more effort at the pre-detailed phase in order to prevent the selection of an unsatisfactory concept early in the design process. Considering the impact of the turbine tip clearance on an engine's efficiency, an accurate tool to predict the tip gap is a mandatory step towards the implementation of a full PMDO system for the turbine design. Tip clearance calculation is a good candidate for PMDO technique implementation considering that it implies various analyses conducted on both the rotor and stator. As a second step to the development of such tip clearance calculator satisfying PMDO principles, the present work explores the automation feasibility of the whole analysis phase of a turbine shroud segment and housing assembly preliminary design process, and the potential increase in the accuracy of results and time savings. The proposed conceptual system integrates a thermal boundary condition automated calculator and interacts with a simplified air system generator and with several design tools based on parameterized CAD models. Great improvements were found when comparing this analysis method results with regular pre-detailed level tools, as they revealed to be closer to the one generated by the detailed design tools used as target. Moreover, this design process revealed to be faster than a common preliminary design phase while leading to a reduction of time spent at the detailed design phase. By requiring fewer user inputs, this system decreases the risk of human error while entirely leaving the important decisions to the designer.

Keywords Preliminary and Multidisciplinary Design Optimization, Shroud Segment, Tip clearance, Automated analyses

1. Introduction

The design of a gas turbine engine is a multidisciplinary and iterative problem in which the best compromise has to be found between the conflicting disciplines involved: thermal, structural, aerodynamics, manufacturing, cost, weight, etc. The design of aero-engines traditionally follows two main stages: preliminary design and detailed design. At the pre-detailed stage, only a few groups are involved to design and analyse the turbine concept's components and sub-systems. However, the Science and Technology Organisation of the North Atlantic Treaty Organization (NATO) [1] showed that decisions taken early in the design process are often based on low fidelity models when only little information (data, requirements, etc.) is available. This may compromise the analysts' ability to select the optimal design. At the detailed design phase, more groups are involved having their own set of specialized tools and

methodologies, and the process is thus even more segmented within the groups to form sub-disciplines' specialists. Panchenko et al. [2] explain that even though knowledge increases during the design process, the freedom to modify any part of the design decreases as shown in Fig. 1, and/or induces major delays in the planning and a rise of design costs. It is consequently difficult to correct a bad concept at a detailed design phase. To correct this, Panchenko et al. [2] suggest the use of MDO at the preliminary design phase, since it is at that stage that the biggest influence on the final product configuration can be made. As explained by Martins and Lambe [3], the concept of MDO has been widely studied during the past 50 years. However, there is a lack of information in the literature about using this methodology during the early stages of design. Pachenko et al. [2] explain that an increase of the effort and knowledge during the pre-detailed design phase implies involving directly the specialist groups instead of waiting until the detailed design phase. However, it results in significant delays of the concept evolution since many interactions between several groups are then required. This is where PMDO systems come into play in order to automate and ease this iterative process. Referring to Pachenko et al. [2], NATO Science and Technology Organisation [1] and Korte et al. [4], the following steps are required to implement a PMDO system:

* Corresponding author:

Francois.Garnier@etsmtl.ca (F. Garnier)

Published online at <http://journal.sapub.org/aerospace>

Copyright © 2019 The Author(s). Published by Scientific & Academic Publishing

This work is licensed under the Creative Commons Attribution International

License (CC BY). <http://creativecommons.org/licenses/by/4.0/>

1. Develop a robust tool base: design tools based on parametrized CAD models, and advanced physics analysis tools which includes the development or improvement of correlations;
2. Apply single discipline optimization to individual analytical tools;
3. Create an integration framework, i.e. a software architecture enabling integration, communication and execution of several tools;
4. Implement multidisciplinary optimization with a clear statement of the design objectives, constraints and variables, and an appropriate selection of the algorithms.

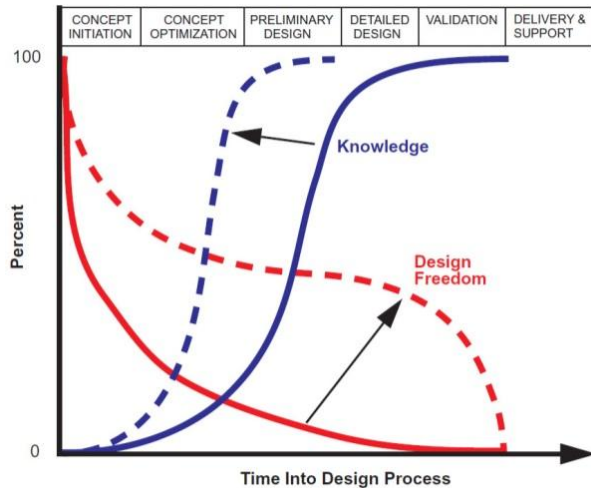


Figure 1. Knowledge vs. design freedom during the design process. Knowledge increases during design process (solid line to dash line) while design freedom decreases (solid line to dash line) [1]

A collaborative program was initiated between Pratt & Whitney Canada and the École de Technologie Supérieure to implement an MDO system for designing turbines at the pre-detailed design phase (PMDO). The present work focuses on the second part of the first step described here

above (i.e. the analysis portion) and on the second and third steps. As part of this collaborative program, the development of a tip clearance calculation system is a mandatory step and a perfect example for the implementation of a PMDO methodology considering that it requires the design and analyses (thermal, structural and aerodynamic) of several turbine components as described in Fig. 2. Lattime and Steinetz [5] show that the prediction of a turbine's tip clearance through a typical flight mission is essential in order to maximize an engine's efficiency and its service life. Indeed, an increase of the tip clearance implies that the engine has to augment the turbine inlet temperature to develop the same thrust. If the disk temperature reaches its upper limit, the engine must be removed for maintenance. If the gap between the rotor and the shroud segments is larger than 1% of the blade's height, an increase of 1% in tip clearance produces a drop of about 1% in efficiency, according to Hennecke [6]. Based on this, a process for prediction of tip clearance size variation is mandatory in an integrated turbine design system.

In order to develop a tip clearance calculator at the preliminary phase using PMDO principles, three steps can be identified: (1) the prediction of the rotor's thermal and centrifugal growth (already published in [9]); (2) the prediction of the static components' thermal growth (subject of this article); and finally (3) the calculation of the radial gap between the blade tip and the shroud segment (subject of a following article). As introduced here above, this paper focuses on implementing an automated process to analyze the housing (or casing) and shroud segment (also called blade outer air seal) assembly, referred to as "stator" in this work.

Savaria *et al.* [10] worked on the development of the stator design module used as a base for the present work. Fig. 3 shows an example of stator assembly and introduces the naming convention used in this paper for each components of the stator geometry.

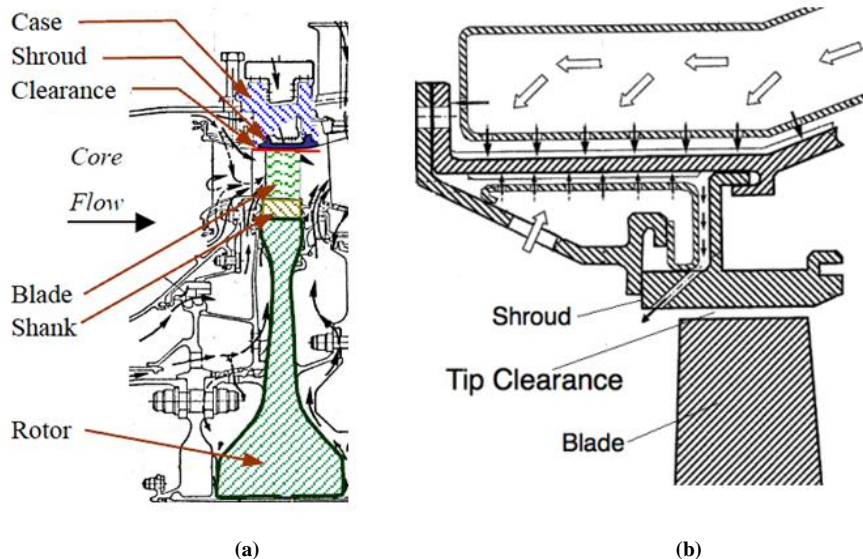


Figure 2. (a) Geometry of the E³ high-pressure turbine [7]; (b) Highlighting of the tip clearance [8]

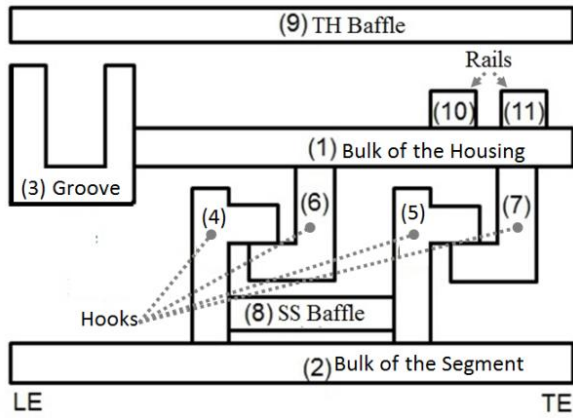


Figure 3. Stator Assembly Components Names [10]

This work is structured as follows. The Methodology used to implement the solution is first presented. After that the Secondary Air System Generation chapter develops the automatic creation of a numerical fluid network. The Thermal Boundary Conditions calculation process is then introduced, including the simplifications and assumptions made for the heat transfer coefficients calculation. This is followed by a chapter on the Automated Analyses which develops how each part of the process communicates with each other. Finally, the paper concludes with a presentation of the main results allowing validating the proposition made in this work by meeting the stakeholders' criteria.

2. Methodology

Based on Wieringa's definition [11], this work is a practical problem as opposed to a knowledge problem. Therefore, the goal of this work is to identify the requirements of the industry regarding the research problem, to propose a new process in response to those requirements, and to implement that proposal. The initial requirements were to improve the pre-detailed design process by proposing a more flexible, robust and adaptable design and analysis system. This means that the new system has to allow more stator configurations to be modeled while requiring limited number of input from the user. Moreover, the new process results should be targeting within 20% accuracy when compared to detail design results. This 20% difference comes from the fact that, based on experts' opinion, it is usually accepted for a regular pre-detailed phase to be about 30% off when compared to the detail design phase results. This target of 20% therefore represents an improvement of 10% compare to the current pre-detailed design process. Finally, the whole design and analysis process should not be slower than the current process.

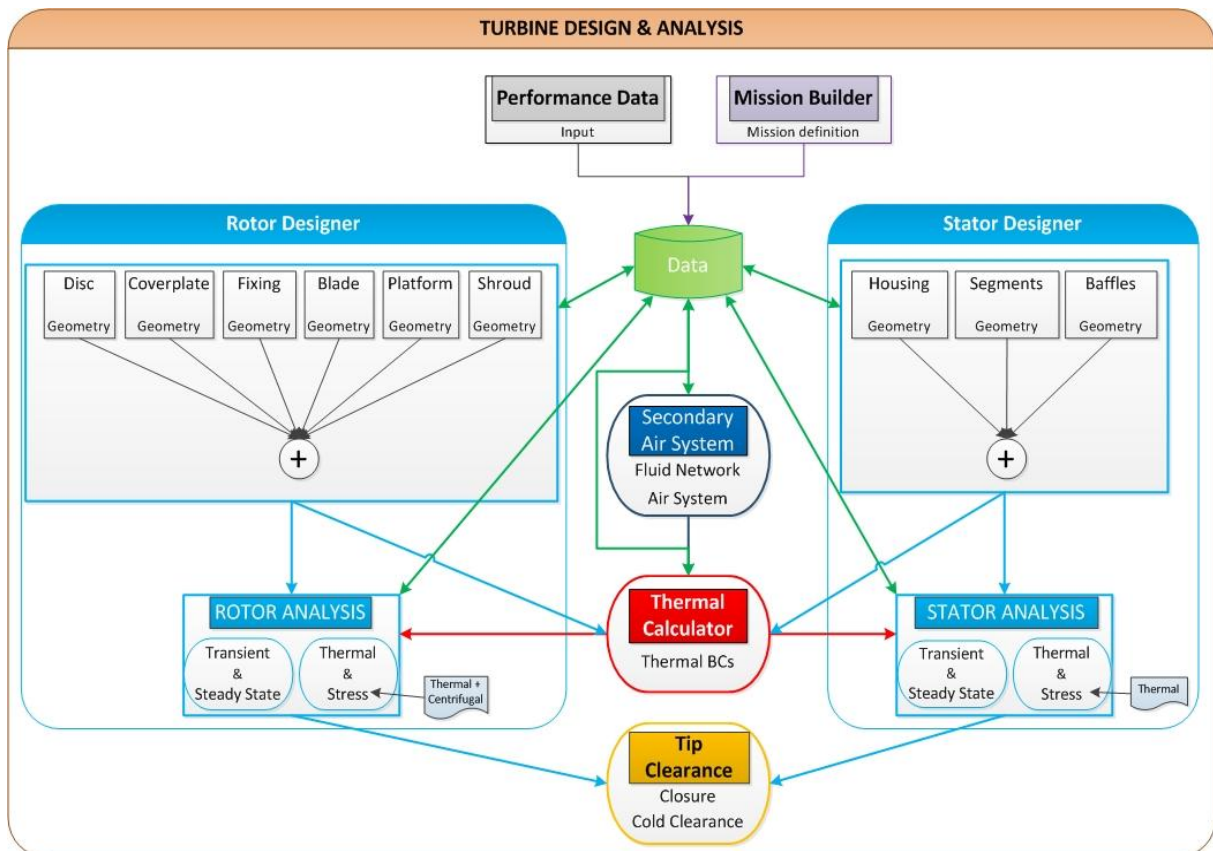


Figure 4. Tip clearance calculation methodology [9]

As it has been developed by the authors previously reported in [9], and is resumed here for the reader's benefit, tip clearance calculation over an entire flight mission implies the determination of the transient radial growth, due to temperature and rotational speed (for the rotor), of the turbine's rotor and static components. Fig. 4, first introduced in [9], shows the architecture of the tip clearance calculation process being developed in this work, where each arrow represents data exchange. As one can see, the creation of a rotor analyses system is the first step toward the implementation of a tip clearance calculator [9]. The present paper investigates the development of the automated analyses process for the housing and shroud segment assembly. The process required in order to evaluate the stator's components displacement includes several sub-systems: pre-processors, an analysis system and a post-processor for visual purposes. The first and highest-level pre-processor sub-system in this program architecture provides the initial concept's data, i.e. the performance data. The second one, called mission builder, generates the flight mission with the proper transient responses to a change in throttle position for all the air chambers around and inside the stator, and in the gas path. The third one is the design tool generating geometric data of the stator based on parameterized CAD models. The sub-systems introduced so far are not the work of the authors. They are indeed developed in the collaborative program initiated between Pratt & Whitney Canada and the Ecole de Technologie Supérieure. Examples of such works are described in Savaria *et al.* [10] for the implementation of the stator designer sub-system or in Ouellet [12] and Twahir [13] for the rotor design sub-systems. The scope of this paper is indeed limited to the following sub-systems as described in Fig. 4.

The fourth sub-system creates the Secondary Air System (SAS) (in dark blue in Fig. 4) based on the stator's configuration, i.e. location of the housing groove, presence of a piston ring in the groove, presence of impingement baffles, number of housing rails, etc. This sub-system is described in the first sub-chapter of this Methodology on Secondary Air System Generation. The final pre-processor sub-system calculates the thermal boundary conditions, i.e. the heat transfer coefficients, for each zone around the stator. This last pre-processor sub-system is described in the sub-chapter on Thermal Boundary Conditions. The Stator Analysis sub-system automatically executes the thermal and stress transient analyses in a CAE software and provides the user with temperature maps and stator displacements. The sub-chapter on Automated Analyses is dedicated to this analysis sub-system. The integration of all these sub-systems is handled by the use of a common and centralized data structure, and by means of object oriented programming (OOP) to create a framework repeated through all parts of the system.

If one assumes that the stator's and rotor's geometries (delivered by sub-systems such as described by Savaria *et al.* [10], Ouellet [12] and Twahir [13]) and the aircraft operating

conditions (i.e. its flight mission) are known, the remaining work in the preprocessing step of a stator's thermal and stress analyses is the generation of the secondary air system and the calculation of the thermal boundary conditions.

3. Secondary Air System Generation

Studying the secondary air system of the stator assembly is important in order to control the thermal growth of the housing (Hennecke [6]) and to maximize the turbine durability by avoiding hot gas ingestion that could lead to metal damage as presented by Malak [14]. Cooling the shroud segment assembly also allows lowering the housing temperature and therefore controlling more easily its thermal growth. Such process is described by Hennecke [6] as a passive system to control the tip clearance variation in the sense that it allows to achieve a slower response of the housing similar to that of the rotor. The shroud segment serves as a thermal barrier taking most of the heat from the gas path and therefore protecting the housing which drives the stator's total growth.

In order to cool the stator, different solutions are used. But the most common ones are to flow the housing with compressor discharge air and to add impingement holes. The housing and shroud segment assembly's geometry can significantly vary from one configuration to another. And the cooling means chosen can also differ for a given geometry. The secondary air system will indeed vary depending on the presence of impingement holes and the number of rows of holes, if a piston ring is sealing a cavity, the orientation of the hooks, the length of a channel, the presence of protuberances, etc. This means that the resulting secondary air systems are very different from one engine to another. A tool automatically generating a fluid network for a given geometry and cooling scheme must therefore be highly flexible.

The Secondary Air System Generator automatically assigns the correct number of air chambers at the relevant locations around the stator, and the stator geometry dictates the type of restrictors to be used between these chambers. The Secondary Air System Generator creates a simplified air system network and provides the necessary inputs to an integrated in-house air system analysis software. Fig. 5 presents three examples of stator with their fluid network automatically generated by the proposed system. The first geometry has a piston ring in the housing groove. The presence of this piston ring seals the cavity above the housing and small leakage flows are modeled passing above and below the ring. One impingement hole also exists in the housing to cool down the shroud segment. The second stator has two impingement holes in the housing central groove with angles different from 90°. The third stator has an impingement baffle attached to the shroud segment. This feature allows reducing the impingement height and therefore increase the heat transfer, but as for drawback to limit the amount of flow that can be used to impinge the shroud segment surface. The third stator is also the only

shown here that has impingement on the housing base itself. The yellow triangles at the extremities of the fluid networks are the air sources constraining the thermal model. Two are located upstream and downstream of the housing and provide cooling air, and two are located in the gas path upstream and downstream of the shroud segment. The third test case has two extra sources above the housing baffle to model the chambers upstream of the impingement holes.

As an example of the use that can be made of this Secondary Air System Generator, the impact of increasing or decreasing the amount of flow used to cool the shroud segment by impingement was studied. Secondary air systems were generated with increasing amount of air impinging the shroud segment base from 0% (meaning no impingement jet but cooling through channel flow instead) of the reference impingement flow from the detail design analysis to 500% of that reference flow. The stator temperatures obtained after thermal analyses run based on the generated secondary air systems were measured and averaged on the shroud segment and housing. These temperatures are non-dimensionalized using the detail design reference temperature of the housing at the reference impingement flow. As one can observe in Fig. 6, the temperatures of both the housing and shroud

segment follow the same pattern. They both decrease significantly when increasing the impingement flow from 0% to 100% of the detail design reference flow. Beyond that point, the temperature of the housing does not decrease much as the flow is increased further more. The shroud segment's temperature continues decreasing linearly with a steeper slope than the housing one. However, the decreasing rate of the shroud segment temperature is also much lower past 100% compared to what it is prior to that point. This means that an optimal value can be found between the stator's temperatures (and therefore radial growth) and the amount of flow used for the impingement of the shroud segment. Minimizing the air used is important as it is extracted from the compressor and therefore represents a loss from an engine's efficiency point of view.

Following a similar procedure, the Secondary Air System Generator allows studying the need for any other geometrical or cooling features that can be created in the stator design tool by rapidly obtaining their impact on the stator temperatures and radial growths. A user can for example add a baffle on the shroud segment and measure the difference in the obtained results. Based on these results, one can decide if there is a need for that extra feature.

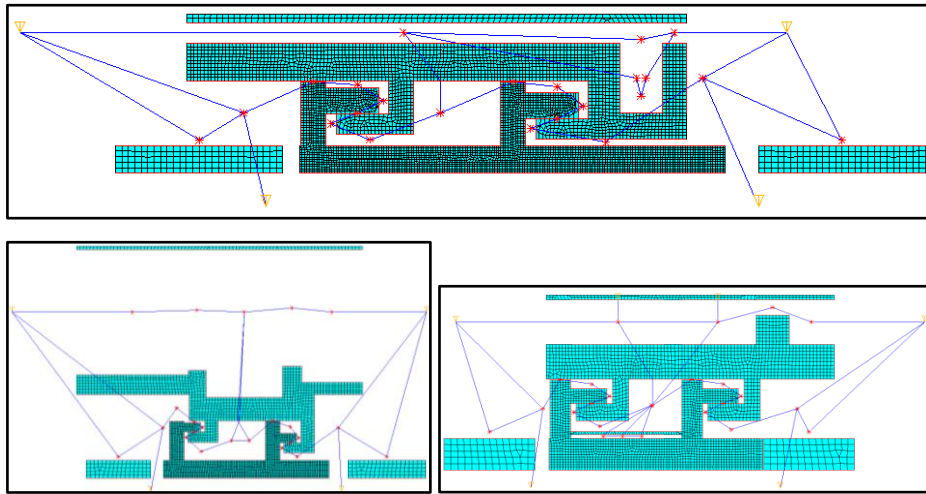


Figure 5. Examples of Secondary Air System

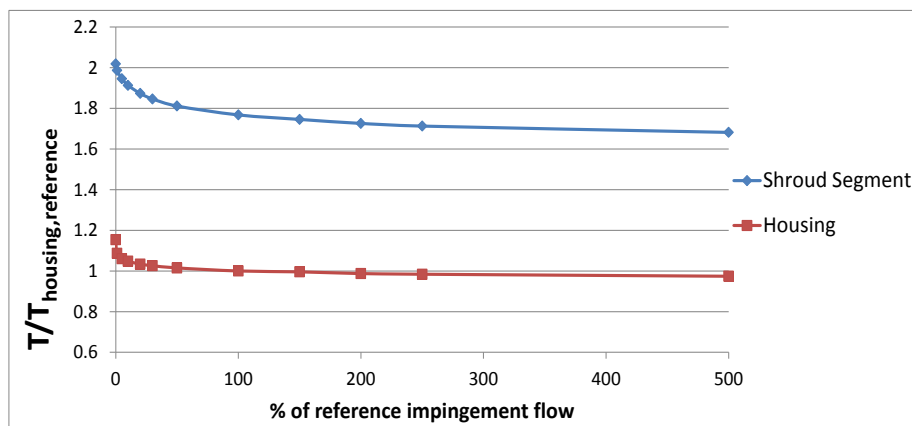


Figure 6. Impingement flow effect on the Shroud Segment and Housing average temperatures

4. Thermal Boundary Conditions

To execute a thermal analysis, boundary conditions are required for each specific location (i.e. zone) around the geometry. The Thermal Calculator uses for each zone a specific set of inputs obtained from all the connected sub-systems (performance data, design CAD sub-systems, the Secondary Air System Generator, etc.) to calculate the thermal boundary conditions. Thanks to a Gateway software, i.e. a link through which two programs can communicate, the Stator Analysis CAE sub-system is able to make use of the CAD parametric models (cf. Savaria *et al.* [10] for example) to identify and measure each zone of the stator geometry.

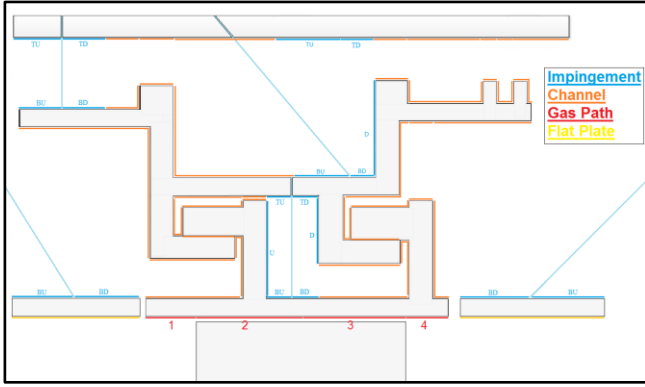


Figure 7. Stator thermal zones

In detailed design, specific correlations are used to evaluate the boundary conditions on a large number of zones defined all around the 3D geometry of the stator to better represent the effect of every seal, hole, cavity, etc. At a pre-detailed level, the 2D geometry is much simpler and therefore fewer zones are defined. It was decided to define one zone per air chamber. Apart from modeling the entire housing and shroud segment assembly, it was decided to represent the tip portion of the upstream and downstream vanes in order to take into account some heat pickup from the fluid network on the sides of the stator. An example of zone distribution around a stator's geometry is presented in Fig. 7 along with the type of correlation used for each of these zones. The thermal boundary conditions correspond to a heat transfer coefficient defined at the surface of each zone, which are also connected to a fluid node. The fluid network connecting every fluid node is constrained by temperature source nodes at the extremities of the network as explained previously and shown in Fig. 5. The zones in the gas path are not connected to a fluid node and have for thermal boundary conditions a combination of a heat transfer coefficient and a bulk temperature at their surface. Kreith *et al.* [15] explain how the bulk temperature can be evaluated based on the fluid's static temperature, its relative velocity and the Prandtl number. Static temperatures around the stator are easily computed based on the gas path mean line temperature (which is part of the initial concept data). The real challenge here is therefore to select the proper correlations for the heat transfer coefficients all around the stator considering that

these are directly influenced by the zone's geometry and the physics at stake. The Nusselt number is often used to evaluate the heat transfer coefficient of a surface as these two are directly correlated. At a preliminary design stage, the zones around the stator can be modeled using basic textbook correlations such as flat plates, channels, impingement, etc. The types of assumptions developed here are represented in Fig. 7.

4.1. Channels

The heat transfer process of channel flows is well known and has been widely covered in the literature (as for example in Incropera and DeWitt [16] or Kreith *et al.* [15]). Channels are present all around the stator geometry and represent the majority of the cooling means used to control the housing temperature. However, some very narrow channels can exist in a stator's geometry (i.e. housing and shroud segments hooks, the piston ring, etc.) for which a simple channel correlation would lead to unrealistically high heat transfer coefficients because of their small hydraulic diameters. Indeed, based on Mehandale *et al.* [17], some of the channels modeled during the boundary condition calculation are in the range of the meso channels (100 μm to 1 mm). For this type of channels, Wang and Peng [18] consistently obtained Nusselt numbers lower than the ones calculated using Dittus-Boelter Eq. (1) [19]. Wang and Peng [18] came up with Eq. (2) which has a reduction factor of 0.35 compared to a regular channel flow correlation (1).

For a turbulent flow in regular channels Incropera and DeWitt [16] and Kreith *et al.* [15] both suggest the use of the Dittus-Boelter Eq. (1) [19]. If the conduit is short and the fluid turbulent, the flow cannot be considered as fully developed and an entrance effect must be accounted for by including a term in the correlation as shown in Eq. (3). In the case of laminar flows the empirical Eq. (4) [20] is suggested.

$$Nu = 0.023 Re^{0.8} Pr^{1/3} \quad (1)$$

$$Nu = 0.00805 Re^{0.8} Pr^{1/3} \quad (2)$$

$$Nu_{with\ entrance\ effect} = Nu \cdot \left(1 + \left(\frac{D_h}{L}\right)^{0.7}\right) \quad (3)$$

$$Nu = 1.86 \left(\frac{Re Pr D_h}{L}\right)^{1/3} \quad (4)$$

4.2. Impingement Jets

Cooling impingement jets are commonly used to provide high local heat transfer in modern gas turbine engine and effectively cool down a specific region of the geometry. Goldstein and Franchett [21] experimentally determined the heat transfer to a jet impinging at different spacing and angles to a plane surface. The authors obtained the empirical correlation Eq. (5) for the local Nusselt number on the plane surface.

$$\frac{Nu}{Re^{0.7}} = A e^{-(B+C \cos\phi)} \left(\frac{r}{D}\right)^{0.75} \quad (5)$$

In Eq. (5), D is the jet diameter, r and ϕ are the cylindrical coordinates of contours of constant Nu and the

coefficients A , B and C are given in the Table 1 depending on the impingement angle α and the distance L from jet orifice to surface. Compared to other research work done on the heat transfer process of impingement jets, using Goldstein and Franchett [21] correlation (5) allows taking into account the effect of the impingement jet's angle which is necessary in housing and shroud segment assemblies where the hardware design often require the use of non-vertical impingement jet.

Table 1. Goldstein and Franchett coefficients [21]

α	A			B	C
	L/D = 4	L/D = 6	L/D = 10		
90°	0.159	0.155	0.123	0.37	0
60°	0.163	0.152	0.115	0.4	0.12
45°	0.161	0.146	0.107	0.47	0.23
30°	0.136	0.124	0.091	0.54	0.34

In their study, Van Treuren et al. [22] realized that when surrounded by crossflow, which is often the case in a stator assembly where channel flows are omnipresent, two heat transfer areas could be defined: the first area being driven by the impingement jet and the second being the area of crossflow influence. These two areas are illustrated in Fig. 8. Van Treuren et al. [22] suggest defining the area of influence of an impinging jet as the region where the Nusselt number values are above 50% of the stagnation point value. However, when automating an analysis process, one needs to define the zone affected by an impinging jet prior any analysis. When using Goldstein and Franchett [21] contours of constant Nusselt number, one can measure that 50% of the Nusselt number at the stagnation point for an angle of 90° correspond to a distance of about 3.125 times the hole diameter from the stagnation point. If measuring this length of influence for the downstream side of the stagnation point depending on the angle of impingement, one comes up with Table 2.

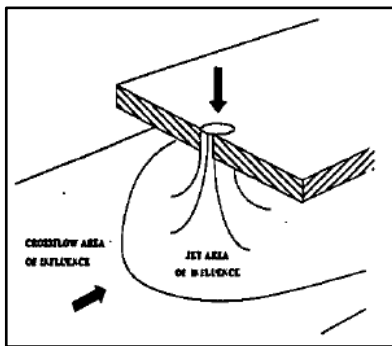


Figure 8. Areas of Influence for the Impinging Jet Array: Jet and crossflow areas of influence [22]

In Table 2, the values for the angles of 120°, 135° and 150° were obtained by using the length of the upstream side (i.e. right of the stagnation point) of the contours for the angles of 60°, 45° and 30° (respectively). When executing a polynomial regression on Table 2, one obtains the Eq. (6) that has an R^2 of 0.9924.

Table 2. Length of influence for an impingement jet

Angle [°]	x/D @ 50% Nu
30	6.875
45	5.938
60	4.375
90	3.125
120	2.375
135	2.187
150	1.563

$$\frac{x}{D} = -3 \cdot 10^{-6} \alpha^3 + 0.0012 \alpha^2 - 0.1689 \alpha + 11.093 \quad (6)$$

The impingement zones are therefore defined by calculating the length of influence of the impingement jet upstream and downstream of the impact point. The zones surrounding the impinged surface and inside the area of influence may not be directly impinged but they are still influenced by the impingement jet heat transfer coefficients due to the jet reflection. Heat transfer coefficients on these zones are generally defined as a percentage of the directly impinged zone's heat transfer coefficient depending on the quantity of cooling flow reflected toward them. This can be observed in Fig. 7 where the second impingement jet (oblique) on the housing groove has five zones affected by the jet: the two zones directly upstream and downstream of the jet (BU and BD), the zone on the right sidewall of the groove (D) which is in the area of influence of the jet and the two zones above the impingement jet (TU and TD). On the other hand, the first impingement jet (vertical) on the housing does not have a zone on the nearest sidewall because this one is outside of jet area of influence.

4.3. Flat Plates

For the sake of simplicity, the gas path side of the vanes can be modeled as flat plates. For such model, Incropera and DeWitt [16] give the following Eq. (7) and (8).

$$\text{Laminar: } Nu = 0.332 Re^{1/2} Pr^{1/3} \quad (7)$$

$$\text{Turbulent: } Nu = 0.0296 Re^{0.8} Pr^{1/3} \quad (8)$$

4.4. Shroud Segment Gas Path Side

Many references such as Azad et al. [23] and Prasad and Wagner [24] developed the behavior of the secondary flow within the blade tip and the shroud segment gap. As Prasad and Wagner [24] proved in their study, the unsteadiness of the flow seems to be mostly confined to the gap between the blade tip and the shroud segment. Based on this observation, one can conclude that for a simplification purpose of the problem at stake, the shroud segment gas path side can be separated in two regions:

- The first one is composed of the surfaces preceding and following the blade. These zones are the numbers 1 and 4 in Fig. 7. They are exposed to the main flow and can be modeled as a flat plate (using Eq. (7) and (8)) considering that the blade tip does to affect them.

- The second region is the portion of shroud segment located above the blade tip and numbered 2 and 3 in Fig. 7. The zones of this second region cannot be modeled as easily as for the first region. The reason is that when the blade is underneath the shroud, the shroud – blade’s tip system can be considered as two concentric cylinders, with the shroud a stationary one. While when no blade is under the shroud, this one can be seen as a flat plate as in the first region. To consider these two cases, one can calculate a ratio of the time the shroud segment is facing the tip to the time it is not.

Rademaker *et al.* [25] studied the heat loading of a shroud segment and more specially the effect of the blade tip’s windage and the radial outflow of cooling flow at the blade squealer tip. Their study of the windage effect is interesting for the present work because it highlights the periodic variation of the shroud temperatures with the passing of the blades. The authors introduce an equation allowing them to calculate the reduction factor in thermal loading to the shroud surface. If one considers this concept and applies it to the present problem of calculating the heat transfer coefficient at the surface of the shroud segment, one can come up with Eq. (9).

$$h = \sigma h_{concentric\ cylinders} + (1 - \sigma) h_{flat\ plate} \quad (9)$$

where σ is the time fraction for which the shroud segment is covered by the blades. Using basic geometry as shown in Fig. 9, this time fraction can be calculated using Eq. (10).

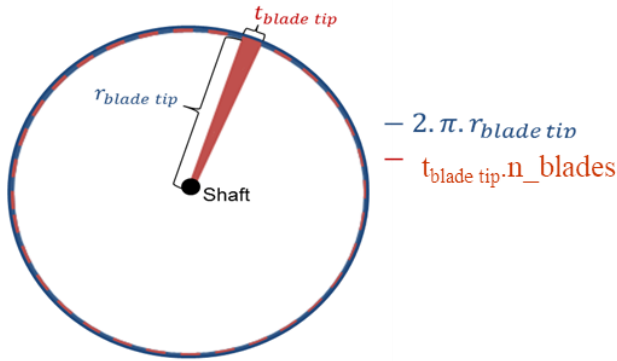


Figure 9. Time Fraction Theory

$$\sigma = \frac{t_{blade\ tip} \cdot n_{blades}}{2 \pi r_{blade\ tip}} \quad (10)$$

where t_{blade} is the blade’s thickness and n_{blades} is the number of blades.

The heat transfer coefficient for concentric cylinders can be calculated using the Dittus-Boelter Eq. (1) [19] but with the Reynold’s number calculated based on the fluid’s relative velocity given by Eq. (11).

$$V_{rel} = \sqrt{U_{rel}^2 + V_{ax}^2} \quad (11)$$

with U_{rel} the fluid’s relative tangential velocity between the two concentric cylinders and V_{ax} the fluid’s axial velocity.

5. Automated Analyses

Automation of the analyses is possible thanks to the process described previously and depicted in Fig. 4. As mentioned previously, the integration of all the sub-systems shown in Fig. 4 is handled by the use of a common and centralized data structure. A framework was created and repeated through all parts of the system by means of object oriented programming (OOP). Automation of the analyses therefore only requires an effective way for the sub-systems to communicate with the CAD and CAE external software. Using a Gateway system, geometric data can be extracted from the CAD parametrized models and used in the sub-systems for calculation and display purposes. This Gateway software also allows direct communication between the CAD models and the CAE software used to run the 2D analyses. The thickness of the non-axisymmetric components (i.e. the shroud segment, and its baffle if any) are calculated based on the number of segments on the circumference, and applied on the meshed geometry in the CAE system.

A program was developed in the CAE software in order to automate the analyses process. Depending on the configuration of the studied stator, this system loads the different components’ 2D geometry from the CAD models. The loaded geometries are meshed using the appropriate elements: thermal, fluid, convection and surface effect elements for the thermal analysis, and structural and contact elements for the stress analysis. The thermal and structural elements are defined as axisymmetric or with thickness depending on the component of the stator they are created for. The calculated thermal boundary conditions, varying in time in accordance with the mission, are applied on the zones identified in the CAE program. Temperatures are set at the boundary nodes of the fluid systems and air flows are applied on the fluid elements around the geometry. For the stress analysis, boundary and load conditions are much simpler to evaluate and apply considering that they consist of axially fixing the housing to prevent any axial translation, and applying the thermal results.

6. Results and Discussion

A 2D transient thermal analysis process is more complex than the following stress analysis. For that reason, the presented results focus on thermals. It is indeed in the thermal analysis part of this work that improvements are made considering that executing a stress analysis is fairly straightforward once thermal analysis results are obtained. Thermal and stress analyses were carried out using the process described in this paper for one turbine stage of three different engines. Those engines are of different configurations: a turboprop as test 1, a turboshaft as test 2 and a high-bypass ratio turbofan as test 3. For all three test cases, this study focused on the first stage of the high

pressure turbine. The results obtained were compared to the final detailed design results used to create these engines. Fig. 10a and Fig. 10b show an example of results obtained for a thermal analysis done on the test case number 1. In Fig. 10b, one can observe the evolution of the temperature probed at five key locations around the stator represented on the temperature contours in Fig. 10a. As absolute values cannot be disclosed in this paper for intellectual property reasons, non-dimensionalized scales were used in Fig. 10a and Fig. 10b. In these two figures, the temperature unit was removed by means of the shroud segment maximum metal temperature and the time scale in Fig. 10b was non-dimensionalized using the Take-off condition's duration.

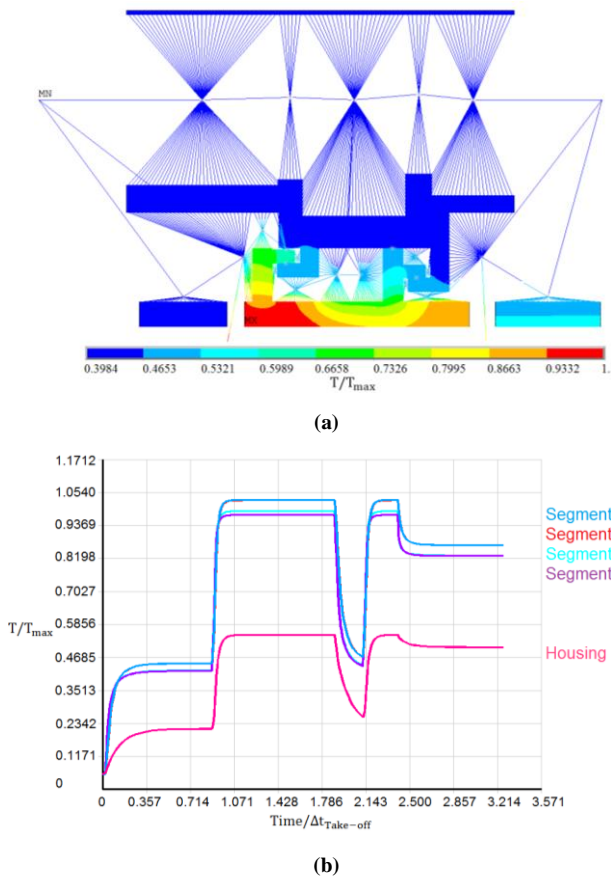


Figure 10. Thermal analysis results example performed on test case 1: (a) contour plot, (b) transient plot of temperatures at key locations

Fig. 11 represents the absolute average difference between the temperatures obtained with the system described in this work and with detailed design level tools. As it does not seem that any conclusion can be made on the over- or underestimation of the temperatures by the pre-detailed design system, absolute values of the differences were used. The temperatures were measured at 10 different key locations around each of the three turbine's stator geometry. The three first locations (in blue) are in the shroud segment base. The four next (in red) are in the hooks (one per hook). And the last three locations are in the Housing base/Groove. One can see in Fig. 11 that results are below (or equal to)

the 20% difference set as target by the stakeholders during the project requirements definition introduced in the Methodology.

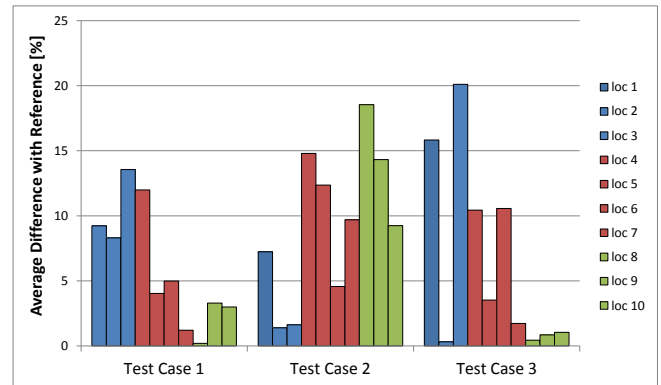


Figure 11. Presented work vs. Detail Design results

Considering that local effects are not of much interest for this study since they do not have a significant influence on the stator radial growth, the results were averaged per component (i.e. the shroud segment, hooks and housing) to highlight the main sources of discrepancies in each test case. Fig. 12 shows these averaged results along with the total differences per component averaged on all three test cases.

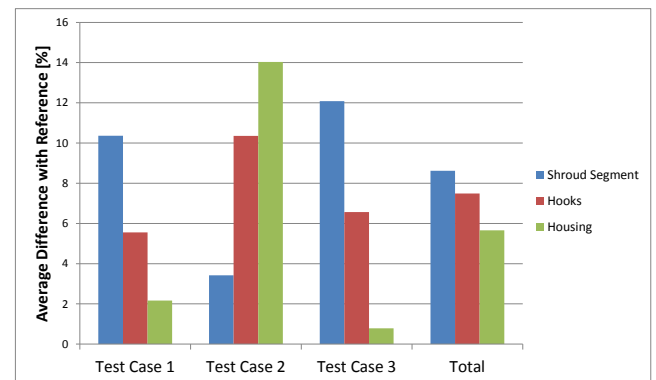


Figure 12. Comparison results averaged per component

One can observe in Fig. 12 that it is in the shroud segment that differences are at a maximum in the first and third test cases. Indeed, an average difference of 10.36% was obtained in the shroud segment of the first test case and an average difference of 12.08% was reached in the same component of the third test case. For the second test case, the Housing is where the differences mainly originate from with an average difference of 14.03%. The total average difference of all test cases for all the components is 7.26%, with a standard deviation of 4.4%, which exceeds the expectations that led to an initial target of 20% difference. However these results can be even more improved if the main source of discrepancies of each test case are studied and answered to.

The shroud segment of the test cases 1 and 3 are internally cooled using channels inside the shroud segment base which conduct air from the shroud/housing cavity downstream of the shroud segment. These channels are modeled in the detail design analysis, but were not part of the initial requirements

of the system introduced in this work. This explains why the results obtained here for the shroud segment base are hotter than the reference detailed design ones. In the second test case, the shroud segment is not internally cooled and the results for the shroud base are much closer to the reference values. However the housing ones are not. This is due to the fact that the detail design analysis models a bigger portion of the geometry of the housing. Indeed, instead of limiting the analysis to the portion of the housing above the shroud segment as it is done in this work, the detail design analysis models the entire housing up to its flange attachment. This leads to a reduced average temperature of the housing by conduction considering that the upstream section of the housing is not affected by any heat from the gas-path.

As a second iteration of the preliminary design process, small modifications were made to the model to better match the reference results. Cooling channels were modeled inside the shroud segment base for the test cases 1 and 3, and a zone was added on the upstream side of the housing of the second test case in order to mimic the effect of conduction through the upstream portion of the component. Fig. 13 shows the results obtained after this second iteration of the preliminary design process. A maximum average difference of 9.2% is obtained in the hooks of the second test case. That result is explained by the use in this work of a simplified geometry and air system as compared to the detailed final design (modeling of leakage flows, definition of extra holes, extra channels and other features for example), which have an impact on the thermal boundary conditions. The second source of difference with the detail design process is the simplicity of the models used for the calculation of the heat transfer coefficients and the number of zones used. However, a difference of less than 10% at the pre-detailed level compared to detailed design results is excellent. Moreover, the average of the differences of the three turbines at all the locations is 3.78% with a standard deviation of 2.5%.

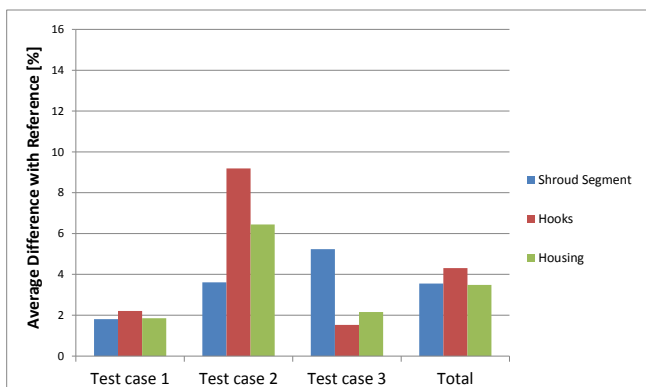


Figure 13. Presented work vs. Detail Design improved results

Comparing the system presented in this work with the existing pre-detailed design process is not easy because the proposed solution goes beyond what is usually expected from a preliminary design phase. Only few data are therefore available that allow comparing the presented solution with both a usual pre-detailed solution and at the same time with

what was finally obtained during the detailed design phase for the same test case. One engine was however identified that went through both these steps using recent methods and analytical tools from beginning to end. The third test case introduced previously allows the authors to measure the improvement brought by the system introduced in this paper by comparing it to the process that it is supposed to replace.

As one can see in Fig. 14, a first iteration (i.e. not the improved results) of the system described in this work delivers more accurate results than the current process when compared to a detail design analysis. For the shroud segment, the authors' proposal is able to deliver results 20% more accurate than the current process. The proposed system also delivers results 5% more precise in the stator hooks, and 2% in the housing. The housing temperatures are predicted with a similar precision by the two systems because the third test case has a simple housing configuration (no groove or piston ring for example) meaning that the current process is able to properly model the physics at stake. But the shroud segment physics is more complex (impingement baffle with several rows of holes, gas path, etc) which cannot be captured by the current process with as much fidelity as the proposed solution.

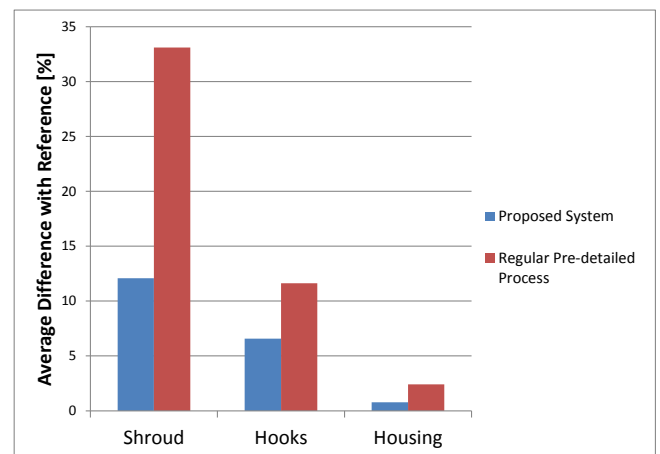


Figure 14. Comparison of the results of the current and proposed processes with detail design results for the test case 3

Starting with an engine concept and the related data, stators were designed and then analyzed using system described in this paper. The time required to execute these studies was compared to what is usually taken by a P&WC expert using the existing pre-detailed design process. Although bringing more knowledge in the early stages of the design process usually increases the time spent at the pre-detailed stage, it was found that the time to get a first pass of results was reduced by 80%. It was indeed evaluated that could now be obtained in days what was usually the result of weeks of work. This improvement comes from the integration of the various disciplines involved in the design and analysis of the turbine's stator, the increased flexibility of the system which removes the need for manual intervention from the user in some parts of the current process, and due to the automation and simplification of the

process (data automatic extraction/generation, reduction of the number of inputs required from the user, etc.).

As introduced in [9], it is expected that with more accurate preliminary results comes a reduction of the number of iterations required at the detailed design phase. It was estimated by several specialists that the detailed design process could be shortened by an entire design cycle. Considering that a detailed design process usually requires on average three iterations of the design cycle, the system introduced in this work could lead to a time reduction of about 30% on the whole housing and shroud segment assembly detailed design phase. This estimation was made on the grounds that a more accurate pre-detailed design, obtained by taking into account more data (i.e. secondary air system, thermals, and even more disciplines incorporated in the other modules of this collaborative program between Pratt & Whitney Canada and the Ecole de Technologie Supérieure), will remove the need for a first pass in the detailed design phase to generate the missing data of a conventional preliminary process.

7. Conclusions

It is expected from the implementation of a PMDO system to improve the quality of pre-detailed level results considering that more knowledge is being injected early in the design process. It is also anticipated that such system would lead to an increase of productivity through the reduction of the overall design time. Through this work it was proved that, when using a PMDO system, the time required to deliver a housing and shroud segment assembly's thermal and displacement results in the pre-detailed design phase is reduced by 80% due to improvements in the process efficiency. It was also estimated that the higher quality and quantity of the pre-detailed data would lead to a time reduction of about 30% during the detailed design phase.

The new system showed a substantial improvement in the quality of the pre-detailed design results, from an estimate of about 30% to less than 8%, when compared to detailed design results. The accuracy of the results was even more improved during a second iteration on the pre-detailed model by adding some extra features to the model, which led to an average difference of less than 4%. These results prove that the decision of reducing the number of boundary condition zones, compared to detailed design best practices, to a minimum of one zone matching each air system chamber is valid. Finally, the selection of simplified models for the calculation of the heat transfer coefficients proved to be valuable when looking at the thermal analysis output.

The results showed in this paper answered the knowledge sub-problem of identifying the predominant phenomena in the thermal analysis of a housing and shroud segment assembly. As expected, the main ones were the impingement jet cooling, the heat transfer from the gas-path, and all the channel flows around the stator. But the system introduced here allowed highlighting the importance of modelling the

cooling channels inside the shroud segment base and the conduction in the housing if it has been cut, which was not initially anticipated.

This work also confirms that an automation of the preliminary design process is possible. The results presented in this paper suggest that one analyst could be in charge of designing and analyzing an entire stator during the pre-detailed phase, without the need for many specialized groups to be involved.

Moreover, by requiring fewer user inputs and removing the non-value added task for an analyst to manage data, this system decreases the risk of human errors while entirely leaving the important decisions to the user.

Finally, the process described in this work closes the gap between the pre-detailed and detailed design phases meaning that results can be generated where assumptions had to be made before.

The next and final stage of this work in order to implement a tip clearance calculator following PMDO principles is to compare the rotor and stator transient displacements in order to identify the most severe pinch point that will define the cold build clearance to be set, and finally to create an optimisation system able to generate an optimal turbine geometry depending on the selected design objectives.

ACKNOWLEDGEMENTS

This work could not have been done without the support of Pratt & Whitney Canada, and the expertise of the employees who helped at the concretization of this project. The authors are grateful for the National Sciences and Engineering Research Council of Canada (NSERC) for partially financing their work.

Nomenclature

CAD = Computer-aided Design
 CAE = Computer-aided Engineering
 D = Impingement jet diameter
 D_h = Hole hydraulic diameter
 h = Heat transfer coefficient
 L = Length of the conduct
 \dot{m} = Mass flow rate
 Nu = Nusselt number
 PMDO = Preliminary and Multidisciplinary Design Optimization
 Pr = Prandtl number
 r = Radius in cylindrical coordinate system
 $r_{blade\ tip}$ = Blade tip radius
 Re = Reynolds number
 $t_{blade\ tip}$ = Blade tip thickness
 U_{rel} = Fluid's relative tangential velocity
 V_{ax} = Fluid's axial velocity
 V_{rel} = Fluid's relative velocity
 x = Length of influence of an impingement jet

$\#_{\text{blades}}$ = Number of blades

α = Impingement angle

ρ = Density of the fluid

σ = Time fraction

ϕ = Azimuth in cylindrical coordinate system

ω = Angular velocity of the co-rotating disks

REFERENCES

- [1] NATO Science and Technology Organization. (2006). *Integration of Tools and Processes for Affordable Vehicles. Chapter 3: Air Vehicles*. NATO RTO Research Task Group AVT 093.
- [2] Panchenko, Y., Patel, K., Moustapha, H., Dowhan, M. J., Mah, S., & Hall, D. (2002). Preliminary Multi-Disciplinary Optimization in Turbomachinery Design. *Proceedings of RTO/AVT symposium on "Reduction of Military Vehicle Acquisition Time and Cost through Advanced Modelling and Virtual Simulation"*, (p. 22). Paris, France: RTO-MP-089.
- [3] Martins, J. R., & Lambe, A. B. (2013). Multidisciplinary Design Optimization: A Survey of Architectures. *AIAA Journal*, Vol. 51(No. 9), 2049-2075.
- [4] Korte, J. J., Weston, R. P., & Zang, T. A. (1998). *Multidisciplinary Optimization Methods for Preliminary Design*. Multidisciplinary Optimization Branch, MS 159, NASA Langley Research Center.
- [5] Lattime, S. B., & Steinetz, B. M. (2004). High-Pressure-Turbine Clearance Control Systems: Current Practices and Future Directions. *Journal of Propulsion and Power*, 20, 302-311.
- [6] Hennecke, D. K. (1985). Active and Passive Tip Clearance Control. *VKI Lecture Series 1985-05*.
- [7] Melcher, K. J., & Kypuros, J. (2003). Toward a Fast-Response Active Turbine Tip Clearance Control. *XVIIth International Symposium on Airbreathing Engines (ISABE)*, (pp. Paper 2003-1102). Cleveland.
- [8] Boswell, J., & Tibbott, I. (2013). *Tip Clearance Control for Turbine Blades*. Rolls-Royce plc. European Patent EP2546471.
- [9] Moret, M., Delecourt, A., Moustapha, H., Abenhaim, A.-I., & Garnier, F. (2017). Automated Thermal and Stress Preliminary Analyses Applied to a Turbine Rotor. *Aerospace Science and Technology*, 123-131.
- [10] Savaria, C., Phutthavong, P., Moustapha, H., & Garnier, F. (2017). New Correlations For High-Pressure Gas Turbine Housing and Shroud Segments. *Aeronautical Journal*, 1-23.
- [11] Wieringa, R. (2009). Design Science as Nested Problem Solving. *4th International Conference on Design Science Research in Information Systems and Technology*, 1-12.
- [12] Ouellet, Y., Savaria C., Roy, F., & Moustapha, H., Garnier, F. (2016). A Preliminary Design System for Turbine Discs. *International Journal of Turbo & Engine jet*. (In press)
- [13] Twahir, A. (2013). Preliminary Design of Blade and Disc Fixing for Aerospace Application using Multi-Disciplinary Approach. *Dissertations and Theses*. Paper 141.
- [14] Malak, M., Liu, J., & Mollahosseini, K. (2015). Further Investigation into Hot Gas Ingestion into Turbine Shroud Cavity Using Uniform Crystal Temperature Sensors Measurement for Baseline Configuration. *22nd International Symposium on Air Breathing Engines*. Phoenix: ISABE.
- [15] Kreith, F., Manglik, R. M., & Bohn, M. S. (2011). *Principles of Heat Transfer* (7th Edition ed.). Stamford, USA: Global Engineering.
- [16] Incropera, F. P., & DeWitt, D. P. (1996). *Fundamentals of Heat and Mass Transfer*. New York: John Wiley & Sons.
- [17] Mehendale, S., Jacobi, A., & Shah, R. (2000). Fluid Flow and Heat Transfer at Micro- and Meso-Scales With Application to Heat Exchanger Design. *Applied Mechanics Reviews*, 175-193.
- [18] Wang, B., & Peng, X. (1994). Experimental Investigation on Liquid Forced-Convection Heat Transfer Through Microchannels. *International Journal of Heat and Mass Transfer*, 73-82.
- [19] Dittus, F. W., & Boelter, L. M. (1930). *Univ. Calif. Berkeley Publ. Eng.*, vol 2, p. 433.
- [20] Sieder, E. N., & Tate, C. E. (1936). Heat Transfer and Pressure Drop of Liquids in Tubes. *Ind. Eng. Chem.*, vol. 28, p. 1429.
- [21] Goldstein, R., & Franchett, M. (1988). Heat Transfer From a Flat Surface to an Oblique Impinging Jet. *Journal of Heat Transfer*, 84-90.
- [22] Van Treuren, K., Wang, Z., Ireland, P., Jones, T., & Kohier, S. (1996). Comparison and Prediction of Local and Average Heat Transfer Coefficients Under an Array of Inline and Staggered Impinging Jets. *International Gas Turbine and Aeroengine Congress & Exhibition*. Birmingham: ASME.
- [23] Azad, G. S., Han, J.-C., Teng, S., & Boyle, R. J. (2000). Heat Transfer and Pressure Distributions on a gas Turbine Blade Tip. *Journal of Turbomachinery*, 122, 717-724.
- [24] Prasad, A., & Wagner, J. (2000). Unsteady Effects in Turbine Tip Clearance Flows. *Journal of Turbomachinery*, 621-627.
- [25] Rademaker, E., Huls, R., Soemarwoto, B., & van Gestel, R. (2013). Modeling Approach to Calculate Redistributions of HPT-Shroud Cooling Channels Minimizing Thermal Stresses Including Some Turbine Blade Tip Effects. *Turbine Blade Tip Symposium*. Hamburg: ASME.